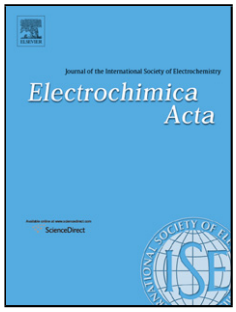


Title: Effect of pH and Water Structure on the Oxygen Reduction Reaction on platinum electrodes

Authors: Valentín Briega-Martos, Enrique Herrero, Juan M. Feliu

PII: S0013-4686(17)30956-8
DOI: http://dx.doi.org/doi:10.1016/j.electacta.2017.04.162
Reference: EA 29420

To appear in: *Electrochimica Acta*

Received date: 31-1-2017
Revised date: 29-4-2017
Accepted date: 29-4-2017

Please cite this article as: Valentín Briega-Martos, Enrique Herrero, Juan M.Feliu, Effect of pH and Water Structure on the Oxygen Reduction Reaction on platinum electrodes, Electrochimica Actahttp://dx.doi.org/10.1016/j.electacta.2017.04.162

# Effect of pH and Water Structure on the Oxygen Reduction Reaction on platinum electrodes.

*Valentín Briega-Martos, Enrique Herrero* and Juan M. Feliu**

Instituto de Electroquímica, Universidad de Alicante

Apdo.99, E-03080 Alicante, Spain

e-mail: herrero@ua.es; juan.feliu@ua.es

**Abstract**

The oxygen reduction reaction (ORR) at different pH values has been studied at platinum single crystal electrodes using the hanging meniscus rotating disk electrode (HMRDE) configuration. The use of NaF/$HClO_4$ mixtures allows investigating the reaction up to pH = 6 in solutions with enough buffering capacity and in the absence of anion specific adsorption. The analysis of the currents shows that the kinetic current density measured at 0.85 V for the Pt(111) electrode follows a volcano curve with the maximum located around pH = 9. This maximum activity for pH = 9 can be related to the effects of the electrode charge and/or water structure in the ORR. On the other hand, the catalytic activity for the other basal planes shows a monotonic behavior with a small dependence of the activity with pH. For stepped surfaces with (111) terraces, the behavior with pH changes gets closer to that of the Pt(111) surface as the terrace length increases. Additionally, the ORR curves show a dependence of the limiting diffusion current with pH. It is observed that the limiting current density diminishes as the pH increases in a potential region where hydrogen peroxide is readily reduced. These results suggest the existence of a bifurcation point in the mechanism previous to peroxide formation, in which $OOH^{\cdot}$ is proposed as the bifurcation intermediate. The reduction of $OOH^{\cdot}$ requires proton addition and would be more difficult at neutral pH values, justifying the diminution of the limiting currents.

**Keywords:** oxygen reduction reaction; ORR; pH effect; water structure; platinum single crystals; Pt(111)

## 1. Introduction

The oxygen reduction reaction (ORR) is the most important cathodic process in fuel cells and one of the most difficult challenges in electrocatalysis, because the reaction involves the transfer of four electrons to form water, the final reduction product. This fact indicates that the mechanism is complex and it implies several elementary steps and intermediates [1]. It is generally accepted that adsorbed O, OH, and OOH are the relevant intermediates in the reaction mechanism, and their interaction energies with the electrocatalytic surface depend on the nature of the material and its surface structure. When the electrocatalytic activity for the ORR is plotted vs. the O binding energy ($\Delta G_{Oads}$) on different substrates, it was found that the points follow a volcano curve [2-4]. Considering this, the design of new catalysts by optimization of the binding energies for the different intermediates would bring to an improved performance for this reaction. Researchers have followed this idea and electrode materials with improved activities with respect to platinum, the best pure metal for this reaction [5], have been obtained [6-8]. However, even for the best performing electrocatalysts, the overpotentials are still significant. Moreover, theoretical studies predict that any further improvement in the ORR performance beyond some given values of these binding energies is impossible because there is

a scaling relationship between the O bonding strength and those of OH and OOH. Reaching the optimal value for the electrocatalytic activity would have required that those binding energies could have been optimized independently. The link between their binding energies [9] leads to a limit in improving the ORR performance by following this strategy.

Analogously, in the case of platinum single crystal electrodes, theoretical studies have pointed out a volcano-type response for the ORR performance as a function of $\Delta G_{Oads}$ or the binding energy of OH ($\Delta G_{OHads}$), being the (111) orientation at the top of this curve [10, 11]. The reactivity of the basal planes with zero defects can be investigated by extrapolation of the ORR activity from stepped surfaces, and contrarily to theoretical results, these experiments show that, in acidic solutions, stepped surfaces are more active than Pt(111) [12-14]. However, in alkaline media, experimental results indicate that Pt(111) is the most reactive surface [15], in agreement with the theoretical predictions. This could be related with the fact that these calculations use surface charge densities more negative than those achieved in $HClO_4$, so it is possible that the surface charges are not appropriately included in the model. This points out that additional studies are required in order to clarify these contradictions.

Beyond the energetics of bonding interactions between the intermediates and the metal surface, interfacial properties such as the electronic distribution in the metal and the water structure affect the catalytic properties of the electrocatalyst. On the one hand, regarding the interfacial charge, the potential of zero charge (pzc) is a parameter of critical importance. This parameter can include the charge involved in adsorption processes, being defined in this case as potential of zero total charge (pztc), or when the true electronic charge is only considered, then called potential of zero free charge (pzfc) [16, 17]. The pztc is usually the accessible magnitude and the pzfc is estimated within a model. The study of the influence of the pH on the total and free charge provides important information about the structure of the interface and the state of adsorbed hydrogen and OH species, as well as possible intermediates, and their influence on the mechanism of the ORR. In previous works, pztc and pzfc have been calculated both in acidic and alkaline solutions for different platinum well-oriented surfaces, mainly using the CO displacement technique [18-22] . Martínez-Hincapié et al. were able to obtain the variation of the pztc and pzfc for Pt(111) within the pH region between 3 and 5, an unexplored pH range until that moment for this type of experiments because the common used buffers employ anions that adsorbs specifically, but the use of $NaF/HClO_4$ mixtures overcame that problem safely [23].

On the other hand, anions can act as modifiers of the water structure. There are two families of anions: kosmotropes (or structure makers) and chaotropes (or structure breakers), according to their relative abilities to induce the structuring of water [24-28]: water is ordered by small or multivalent ions and disordered by large monovalent ions. For example, $Cl^-$ and $F^-$ would be kosmotropic anions, while $ClO_4^-$ and $HSO_4^-$ would be chaotropic anions [27, 29]. A previous work shows that the activity for the ORR on Pt(111) in methanesulfonic acid (MTSA) is slightly lower than the activity in perchloric acid. MTSA is kosmotrope in comparison with $HClO_4$. A stronger liquid water structuring would increase water dipole polarization at the electric double layer and/or decrease the mobility/reactivity of participating non-adsorbed species [29], resulting in a smaller activity.

Despite the significant advances made in the last years from both experimental and theoretical works, many aspects of the reaction mechanism are not totally clear yet. On the one hand, several authors have proposed that the ORR on Pt takes place via the formation of an adsorbed hydroperoxyl radical ($OOH^{\cdot}$) [3, 30-32]:

$$Pt + O_2 \rightarrow Pt - O_2 \quad (1)$$

$$Pt - O_2 + H^+ + e^- \rightarrow Pt - OOH \quad (2)$$

Staszak-Jirkovský et al. proposed a mechanism scheme for the ORR in which adsorbed OOH is a bifurcation point to yield $H_2O$ or $H_2O_2$ as primary reaction products, although the latter can also originate $H_2O$ [33]. This could explain the change from a 4 electrons to a 2 electrons oxygen reduction mechanism in acid media that has been observed for Pt(111) in the potential region where hydrogen is adsorbed [1], since the adsorbed hydrogen atoms would occupy the μ-peroxo adsorption $O_2$ sites, preventing the complete reduction to water and giving thus hydrogen peroxide. Ruvinskiy et al. also considered the intermediate OOH as a bifurcation point, which can be reduced to $H_2O_2$ or decompose to adsorbed O and OH through a chemical step [34].

On the other hand, Gómez-Marín et al. proposed the following mechanism in acidic media in light of the results obtained in experiments with low concentrations of oxygen [35]:

$$O_2 + Pt - H_2O \rightarrow Pt - OH + OOH^{\cdot} \quad (3)$$

$$Pt + OOH^{\cdot} + H^+ + e^- \rightarrow Pt{-}H_2O_2 \quad (4)$$

$$Pt + Pt - H_2O_2 \rightarrow 2Pt - OH \quad (5)$$

$$3 \times (Pt - OH + H^+ + e^- \rightarrow Pt + H_2O) \quad (6)$$

Within this framework, hydroxyl radical, $OOH^{\cdot}$, would be a soluble species interacting strongly with the water network, that can be reduced to $H_2O_2$ or disproportionate into $H_2O_2$ and oxygen in a non-electrochemical reaction. Furthermore, $OOH^{\cdot}$ has a moderate reactivity to decompose, following a second-order dismutation reaction [36], so it can accumulate near the electrode surface and it could be stabilized by the interfacial water close to the electrode surface. In conclusion, $OOH^{\cdot}$ would be an intermediate that could exist in solution or very near to the electrode surface [35]. These previous works indicate that $OOH^{\cdot}$ intermediate could be crucial in the oxygen reduction reaction.

In alkaline media, it is proposed that the ORR proceeds via the formation of a superoxide anion ($O_2^{\cdot-}$) after reaction (1) [37]:

$$Pt{-}O_2 + e^- \rightarrow Pt - O_2^- \quad (7)$$

$$Pt + Pt{-}O_2^- + H_2O \rightarrow Pt - OOH^- + Pt - OH \quad (8)$$

$$Pt - OOH^- \rightarrow Pt - O + OH^- \quad (9)$$

$$Pt - O + H_2O + e^- \rightarrow Pt - OH + OH^- \quad (10)$$

$$2 \times (Pt - OH + e^- \rightarrow Pt + OH^-) \quad (11)$$

Reactions (2) and (7) are generally considered rate determining steps, and adsorbed $OH^{\cdot}$ could act as a poison by blocking available sites for $O_2$. Superoxide anion has been detected as an intermediate of the ORR on Pt in alkaline media by Shao et al. using surface-enhanced infrared reflection absorption spectroscopy with attenuated total reflection (ATR-SEIRAS) [38].

Considering all the mentioned above, a study of the effect of interfacial properties like the pH and electrode charges on well-defined surfaces is mandatory in order to fully understand the ORR mechanism and improve the predictions of the theoretical models. This is important for selecting the best conditions to design new electrocatalytic materials used in fuel cells. Working

at intermediate pH values requires the use of buffered solutions in order to avoid local pH changes at the interphase. Buffer solutions commonly used, for example, phosphate buffer, introduce anions that adsorb specifically, and whose adsorption strength depends on the pH [39]. It is clear then that the study of the effect of the pH and electrode charge should be carried out in the absence of specific adsorption. In order to accomplish that, NaF/$HClO_4$ mixtures concentrated enough to achieve the necessary buffering capacity have been used.

**2. Experimental**

Experiments were carried out in a two-compartment glass cell with three electrodes following the general procedure described in [40]. The working single crystal electrodes were prepared from small Pt beads ca. 2 mm in diameter, following the method described by Clavilier et al. [41]. In this work basal planes, i.e., Pt(111), Pt(100) and Pt(110) electrodes, and stepped surfaces have been used. The selected stepped surfaces have (111) symmetry terraces and (110) or (100) monoatomic steps. These surfaces are Pt(554), Pt(775), Pt(544) and Pt(755), which, according to the Lang, Joyner and Somorjai (LJS) [42] nomenclature correspond to the Pt(S)[9(111)×(110)], Pt(S)[6(111)×(110)], Pt(S)[9(111)×(100)] and Pt(S)[6(111)×(100)] surfaces, respectively. Before each measurement, the working electrode was flame annealed in a propane-oxygen flame, cooled in an Ar/$H_2$ (3:1) atmosphere and transferred to the electrochemical cell protected by an ultrapure water drop saturated with these gases. It has been reported that the cooling atmosphere used in this work give rise to experimental surface structures in agreement with the nominal topographies [43]. Pt(110) surfaces can reconstruct from a (1×1) surface to a (1×2) missing-row surface depending on the cooling method employed. On the one hand, Markovic et al. proposed that slower cooling conditions may lead to the (1×2) surface, while faster cooling would lead to the (1×1) surface [44]. On the other hand, Attard et al. suggested that the (1×1) surface requires stricter control of the cooling conditions, and their results show that this surface can be obtained by cooling in a CO atmosphere [45]. Since the voltammetric profiles obtained with the cooling method presented here are very similar to the presented cyclic voltammetry in [44] for the (1×1) surface, it could be deduced that the Pt(110) surfaces presented in this work are (1×1) surfaces or, at least, mixed (1×1)/(1×2) surfaces with major (1×1) contribution. The counter electrode was in all cases a platinum coiled wire cleaned by flame annealing. The reference electrode used in the case of solutions without NaF was a reversible hydrogen electrode (RHE), while in the case of solutions containing sodium fluoride was a Ag/AgCl, KCl (saturated) electrode.

The exact potential of the Ag/AgCl reference electrode was calibrated by measuring the potential difference between the RHE and the Ag/AgCl electrode, both immersed in a buffer phosphate solution with a well-known pH value. In all cases, the pH of the working solution was measured before and after the experiments to assure that there were no significant pH changes in the solution cell. The measurements showed that the pH changes were always smaller than 0.2 pH units. Potential values have been transformed to the RHE or SHE scale when required.

The working solutions were prepared using concentrated $HClO_4$ (Merck, for analysis), NaF (Merck, Suprapur, 99.99%), $NaOH{\cdot}H_2O$ (Merck, Suprapur, 99.99%), $KClO_4$ (Merck, Suprapur) and ≥ 30 % $H_2O_2$ solution (Fluka, TraceSELECT® Ultra, for trace analysis). Ar, $H_2$ and $O_2$ (N50, Air Liquide) were also employed. Ultrapure water (Elga PureLab Ultra, 18.2 MΩ cm) was used for glassware cleaning and the preparation of the solutions. In the case of solutions with pH values between 2 and 6, the concentrations of NaF and $HClO_4$ were always chosen so that the buffering capacity is high enough to maintain the interfacial pH constant but avoiding the possible contamination that could arise from the glass attack made by generated hydrofluoric acid.

Control cyclic voltammetric profiles were always recorded before and after the ORR measurements, and, in all cases, no noticeable contamination was observed. Experiments with a controlled ratio of oxygen and argon in solution were performed using Smart-Trak® 2 Series 100 Mass Flow Meters and Controllers (Sierra Instruments).

A signal generator EG&G PARC and eDAQ EA161 potentiostat with an Edaq e-corder ED401 recording system were used for the electrochemical measurements. All the experiments were performed with the hanging meniscus rotating disk electrode (HMRDE) configuration using an EDI101 rotating electrode. Rotation rate was controlled by a Radiometer CTV 101. Rotating ring-disk electrode measurements were carried out using a Pine AFMSRXE Electrode Rotator using a rotating electrode with both disk and ring made of Pt, and the measurements were taken with an EG&G Bi-Potentiostat Model 366A and an eDAQ e-corder ED401. All experiments were carried out at room temperature.

**3. Calculations**

3.1 Evaluation of the kinetic current densities ($j_k$) and Tafel slopes

The current densities, *j*, measured for the ORR during a cyclic voltammetry experiment are limited by mass transport since the oxygen reduction reaction is a diffusion controlled reaction. At a certain overpotential value, current density becomes totally controlled by mass transport and reaches a constant value, showing a plateau in the cyclic voltammogram. This current density value is called limiting current density ($j_l$), and, in our experimental conditions, follows the Levich equation [12, 46]:

$$j_l = 0.62nFD^{2/3}\nu^{-1/6}C^b\omega^{1/2} \quad (12)$$

where *F* is the Faraday constant, *D* is the diffusion coefficient of oxygen, *v* is the kinematic viscosity of the solution, $C^b$ is the bulk concentration of oxygen and *ω* is the rotation rate. For a quantitative and comparative study of the catalytic activity of the electrodes, kinetic current densities ($j_k$), that is, current densities that would have been obtained in the absence of diffusion limitations, must be calculated and analyzed. For a first order reaction, the kinetic current density is related with the measured current density (*j*) and $j_l$ according to the equation:

$$\frac{1}{j} = \frac{1}{j_k} + \frac{1}{j_l} \quad (13)$$

Using equation (5), the Koutecky-Levich equation is obtained:

$$\frac{1}{j} = \frac{1}{j_k} + \frac{1}{0.62nFD^{2/3}\nu^{-1/6}C^b\omega^{1/2}} \quad (14)$$

Therefore, kinetic current densities can be calculated by plotting the inverse values of the measured current density as a function of $\omega^{-1/2}$. $j_k$ can also be calculated from a single rotation rate with the following equation using the experimental value of $j_l$ for the selected rotation rate:

$$j_k = \frac{j}{1 - j/j_l} \quad (15)$$

The electrocalatytic activity of each single crystal electrode in the different solutions can be compared by comparing the different kinetic current densities at a fixed potential.

Moreover, Tafel slopes, another important kinetic parameter in electrochemistry, can be obtained as the slope of the curve that results from plotting the potential as a function of log($j_k$).

## 4. Results and discussion

### 4.1 Study of the electrochemical interface in absence of oxygen

#### *4.1.1. Pt(111)*

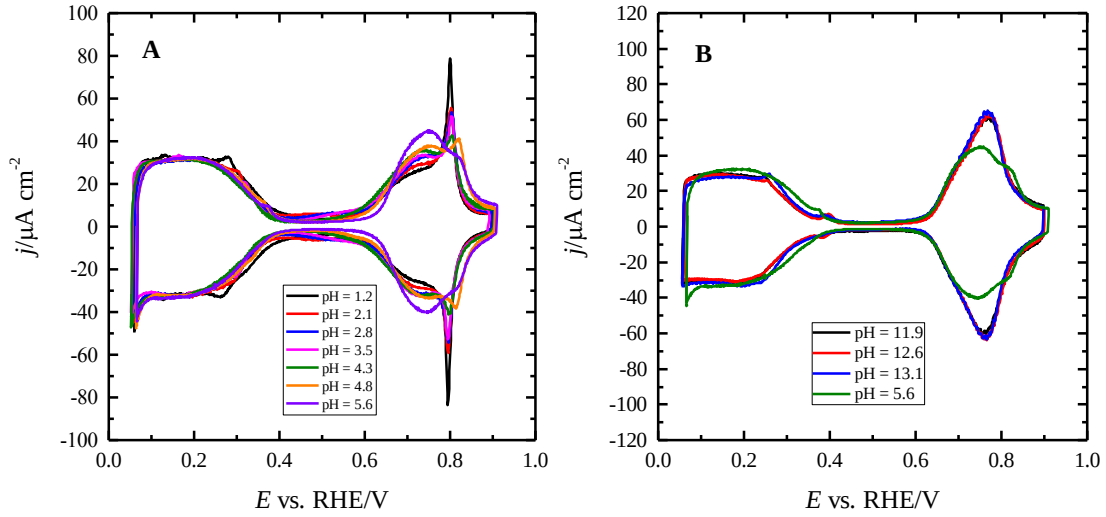


Fig. 1. Voltammetric profiles for Pt(111) in Ar-saturated solutions with pH < 5.6 prepared with $NaF/HClO_4$ mixtures (A) and with pH > 11.9 prepared with $NaOH/KClO_4$ mixtures (B) in the RHE scale. Scan rate: 50 mV $s^{-1}$.

Before studying the oxygen reduction reaction, the metal/solution interphase for the different electrolytes was characterized by means of cyclic voltammetry. Fig.1 shows the obtained results for the Pt(111) electrode in solutions with different pH values in the RHE scale. In 0.1 M perchloric acid, it is accepted that hydrogen adsorption/desorption gives rise to the pseudo-capacitive currents below 0.545 V [47, 48]. The complex voltammetric shape observed between 0.6 and 0.85 V has been assigned to the reversible formation of adsorbed OH. This OH adsorption process has two main features: a broad peak at low potential values followed by a sharp peak at 0.8 V. The complex shape of this part of the voltammetric profile has been explained using two possible alternatives: a random OH adsorption followed by a disorder-order phase transition in the adlayer [49], or an adsorption of OH originated from two different types of water [28]. The obtained cyclic voltammetric profiles for pH values between 2 and 6 are almost identical to those reported in the previous works [22, 23]. It should be highlighted that there are no differences between the voltammetric profiles using $NaF/HClO_4$ mixtures or using only perchloric acid with $KClO_4$ with equal pH and ionic strength [22]. As can be observed,

both H and OH regions lie in the same potential region (in RHE scale) for the different pH values (Fig. 1A). Furthermore, the H and OH adsorption regions are symmetrical in all cases, thus indicating the absence of important local pH variations. Regarding the evolution of the shape of the different regions with pH, while the hydrogen adsorption/desorption region shows minimal modifications as the pH increases, noticeable changes are observed in the OH adsorption/desorption profile. As can be observed, the intensity of the sharp peak in the OH adsorption region at 0.8 V in acidic media decreases as the pH value is increased, while the previous broad signal becomes sharper and more intense. This transformation continues gradually until obtaining the characteristic signal in alkaline media (Fig. 1B). These changes reflect the effects of the absolute electrode potential, that is, the interfacial charge and its

influence on the water structure involved in the OH adsorption process. In conclusion, the use NaF/$HClO_4$ mixtures allows the study of the electrified interface for pH values below 6 without anion adsorption interferences.

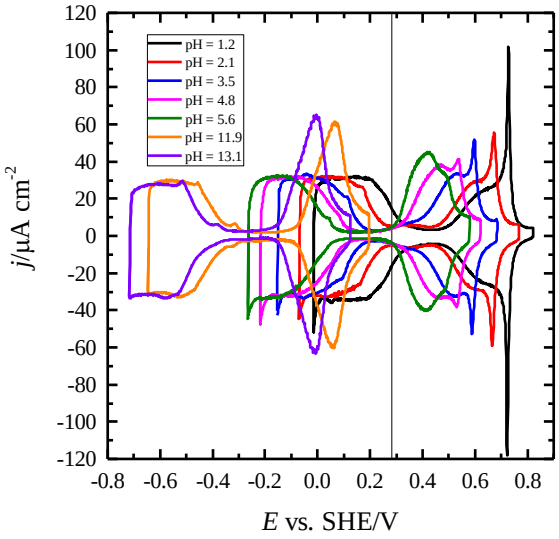


Fig. 2. Voltammetric profiles for Pt(111) in Ar-saturated solutions at different pH values in the SHE scale. Vertical black line indicates the pzfc for Pt(111). Scan rate: 50 mV $s^{-1}$.

The voltammetric profiles plotted in the SHE scale are presented in Fig. 2. This figure allows highlighting an additional feature around 0.35 V (SHE), whose potential does not depend on the pH value. This reversible broad peak is very close to the potential of zero free charge of the Pt(111) electrode (ca. 0.28 V vs SHE), as marked by the vertical line in Fig. 2 [22, 23], and for this reason has been tentatively attributed to the re-orientation of the water dipole layer at the interface [19, 23, 50]. Around pH = 3, pzfc coincides with the pztc implying that, for this pH value, the pztc, which is the directly measurable variable, lies in a region where there is no significant adsorbed OH or H on the electrode surface. Thus, the metal surface at the potential of zero charge is in equilibrium with water molecules directly interacting with the metal surface. For pH values higher than 4, pzfc>pztc and therefore, at the extrapolated value of the pzfc adsorbed OH molecules are present on the metal surface, while for pH lower than 3, pzfc<pztc, an excess of adsorbed hydrogen is present on the interface at the pzfc [22, 23, 51]. It is well known that changes in the surface electrode charge and in water structure can lead to differences in the electrocatalytic activity [1]. These effects will be pointed out in relation to the ORR studies.

*4.1.2. Pt(100), Pt(110) and stepped surfaces*

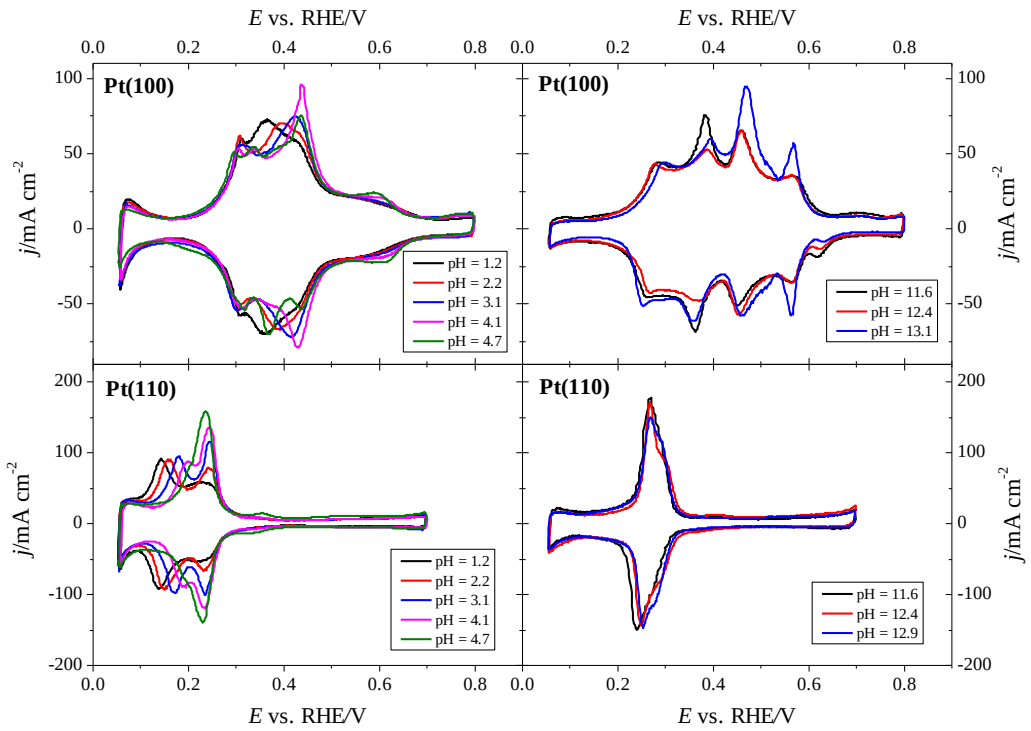


Fig. 3. Voltammetric profiles for Pt(100) and Pt(110) in Ar-saturated solutions with pH < 5.6 prepared with NaF/$HClO_4$ mixtures and pH > 11 prepared with NaOH/$KClO_4$ mixtures in the RHE scale. Scan rate: 50 mV $s^{-1}$.

The other basal planes, namely Pt(110) and Pt(100) surfaces, and the stepped Pt(554), Pt(775), Pt(544) and Pt(755) surfaces have been also studied in this work. The selected stepped surfaces have (111) symmetry terraces with different sizes and (110) or (100) steps. Fig. 3 and 4 show the measured voltammetric profiles at the different pH values. For the Pt(100) electrode, hydrogen and OH adsorption region overlaps [21, 52], so that competitive adsorption processes occur and the shape evolves, as the pH increases, to that obtained in alkaline media [21, 53]. In the case of the Pt(110) electrode, the two peaks observed at low potentials shift to higher potential values and become less resolved as the pH increases. Regarding the stepped surfaces, the peak

traditionally ascribed to H adsorption/desorption at the steps (which appear at 0.13 and 0.26 V in 0.1 M $HClO_4$) [54-56] moves to more positive values in the RHE scale with pH. This is an unexpected behavior because if the adsorption follows the reaction

$$Pt + H^+ + e^- \rightarrow PtH_{step} \qquad (16)$$

the peak should move 0.059 V per pH unit, and therefore it should remain at the same potential value at the RHE scale. Some hypotheses have been proposed to explain this phenomenon, e.g. a mixed contribution of OH and O in this adsorption process [57], changes in the lateral interaction with pH [58] or the oxidative adsorption of water on the step edges [59]. To sum up, the electrochemical interface changes as the pH value is modified for all the studied orientations, and this can have consequences for the ORR activity.

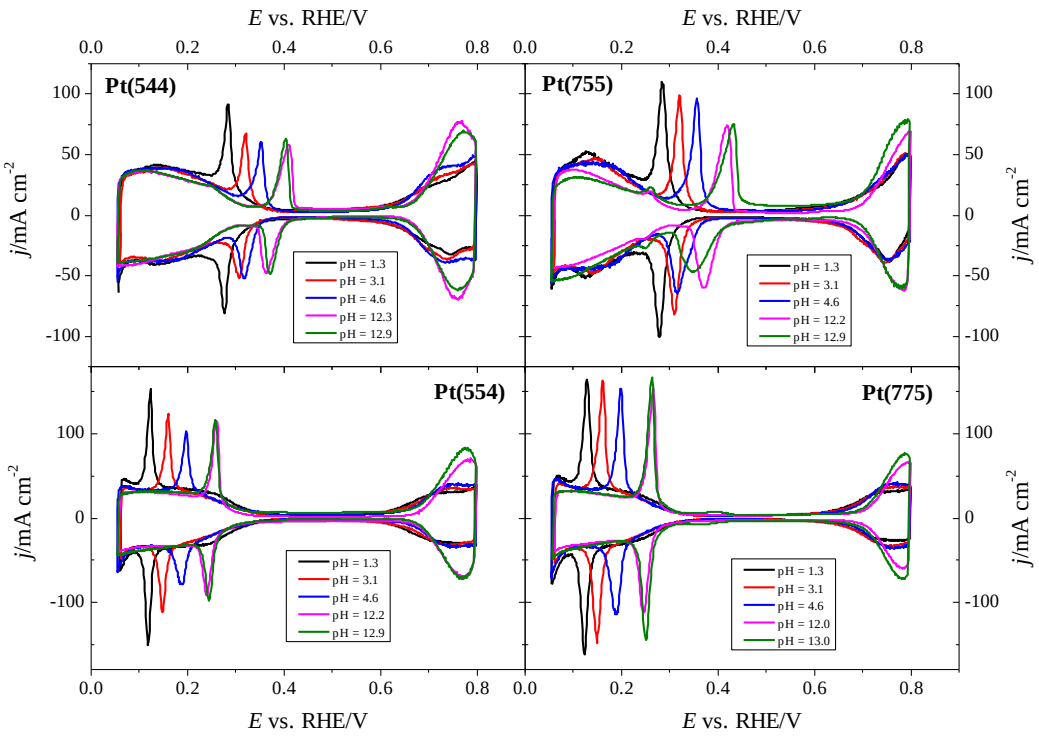


Fig. 4. Voltammetric profiles for different Pt stepped surfaces in Ar-saturated solutions with pH < 5.6 prepared with NaF/$HClO_4$ mixtures and pH > 11 prepared with NaOH/$KClO_4$ mixtures in the RHE scale. Scan rate: 50 mV $s^{-1}$.

## 4.2 Oxygen reduction reaction at different pH values

### *4.2.1 ORR on Pt(111)*

The oxygen reduction reaction has been widely studied in acidic and basic media. However, studies of this reaction in neutral pH values are scarce. The main problem is the difficulty to find a suitable electrolyte without specific anion adsorption and with high enough buffering capacity. Li et al. carried out a study of the ORR on Pt(111) electrodes at different pH values lower than 4 by using small concentrations of $HClO_4$ and increasing the ionic strength with $NaClO_4$ [60]. In this case, the studied solutions are not able to maintain the local pH at the interface. Thus, the observed behavior drastically changes as pH increases when the oxygen reduction reaction takes place. This leads to the apparition of two plateaus in the polarization curves for the ORR: the first one corresponds to the oxygen reduction reaction in acid media (reaction 9), in which the mass transport of $H^+$ is limiting the reaction rate. The second limiting current corresponds to the process in which water molecules are the source of protons, as occurs in alkaline solutions (reaction 10), and with $O_2$ acting as the limiting reagent in this case.

$$O_2 + 4H^+ + 4e^- \rightarrow 2H_2O \; E^0 = 1.23 \text{ V} \qquad (17)$$

$$O_2 + 2H_2O + 4e^- \rightarrow 4OH^- \; E^0 = 0.40 \text{ V} \qquad (18)$$

They analyzed the onset potential before the first plateau and observed that they were very similar. However, there is a remarkable variation of the limiting currents for reaction (9). In this case, when the limiting current is very small, important changes in the onset potential can be unnoticed, because the determination of the onset is very inaccurate. As will be demonstrated,

the use of NaF/$HClO_4$ mixtures allows studying the oxygen reduction reaction in completely buffered conditions provided that the concentration of the electrolyte is high enough. These electrolytic solutions supply more reliable data in order to evaluate the electrocatalytic activity for the ORR at neutral pH values.

Fig. 5 shows the cyclic voltammetric profiles for the ORR on the Pt(111) electrode for pH<5.6 and pH>11.9 in the RHE scale. In general, curves have the typical shape in which the onset is close to 1.0 V, and the limiting current is reached at potential close to 0.75 V. As aforementioned, the absolute value of the limiting current diminishes in the hydrogen adsorption region (below 0.3 V) due to the formation of hydrogen peroxide as final product as described for 0.1 M $HClO_4$ solutions [12, 13, 15, 61, 62]. The first remarkable feature that can be observed is that the onset potential for the oxygen reduction becomes more positive as the pH value of the solution increases for pH<7 (fig. 5A). In other words, the overpotential for the reaction diminishes while increasing the pH, which is the desired aim for the fuel cells technologies, although for practical purposes, it should be considered that solution resistance will increase at low concentrations of $H^+$. Additionally, it is important to highlight that, for pH values higher than 3, the limiting current density between 0.3 and 0.6 V is smaller than the theoretical value, and diminishes as the pH increases. Surprisingly, for pH values around 4, the limiting current density value (in absolute value) increases again around 0.2 V to diminish later close to the onset of hydrogen evolution. This behavior at low potentials is in contrast to that found in more acidic conditions.

On the other hand, for pH>9, the onset potential diminishes as the pH increases. Although cations can affect OH adsorption and the reactivity in alkaline solutions [63], the changes in cation concentration between pH = 11 and pH = 12 are very small (0.099 M $K^+$ + 0.001 M $Na^+$ vs. 0.09 M $K^+$ + 0.01 M $Na^+$), and, in spite of that, there is a clear change in the reactivity, which follows the same trend than that observed for pH = 13 (0.1 M $Na^+$). Moreover, as shown in figure 1, the different concentration of the cation has no effect on the OH adsorption region of the voltammetric profile of the Pt(111) electrode. In addition, an ORR study for Pt(111) at pH ca. 12 has been carried out using a NaOH/NaF mixture, since anion fluoride does not adsorb specifically [23] and hydrofluoric acid is not formed at these pH values. The obtained results are very similar to the results obtained using $KClO_4$ and they follow the same trend. For all the above mentioned, it is considered that the changes in cation concentration are not the origin of these changes. A full kinetic analysis of the curves at different pH values is given in sections 4.2.3. and 4.2.4.

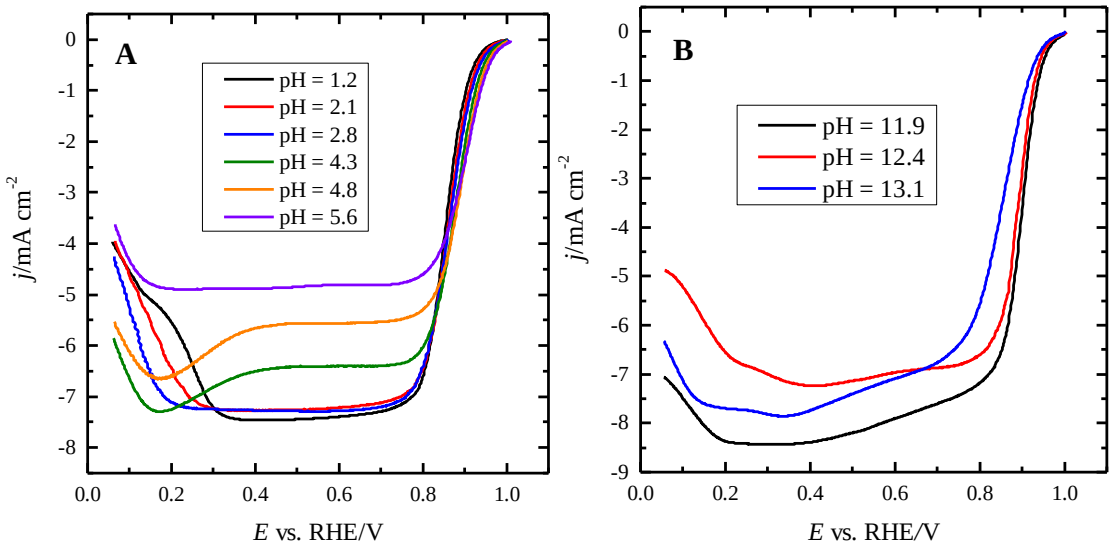


Fig. 5. Polarization curves for the ORR on Pt(111) in $O_2$-saturated solutions with with pH < 5.6 prepared with NaF/$HClO_4$ mixtures (A) and with pH > 11.9 prepared with NaOH/$KClO_4$ mixtures (B). Scan rate: 50 mV $s^{-1}$; rotation rate: 2500 rpm.

*4.2.2. ORR on Pt(100), Pt(110) and stepped surfaces*

The ORR has been also studied for the other basal planes and for stepped surfaces. Results are shown in Fig. 6 and 7. Unlike the Pt(111) electrode, the onset potential in the case of the Pt(100) and the Pt(110) surfaces does not change noticeably. For the stepped surfaces is difficult to observe the trend by only examining the cyclic voltammetric profiles, but a detailed kinetic studied will be presented in section 4.2.3. In general, the diminution of the limiting current is observed for all the surfaces, however in a lesser extent than that observed for the Pt(111) surface.

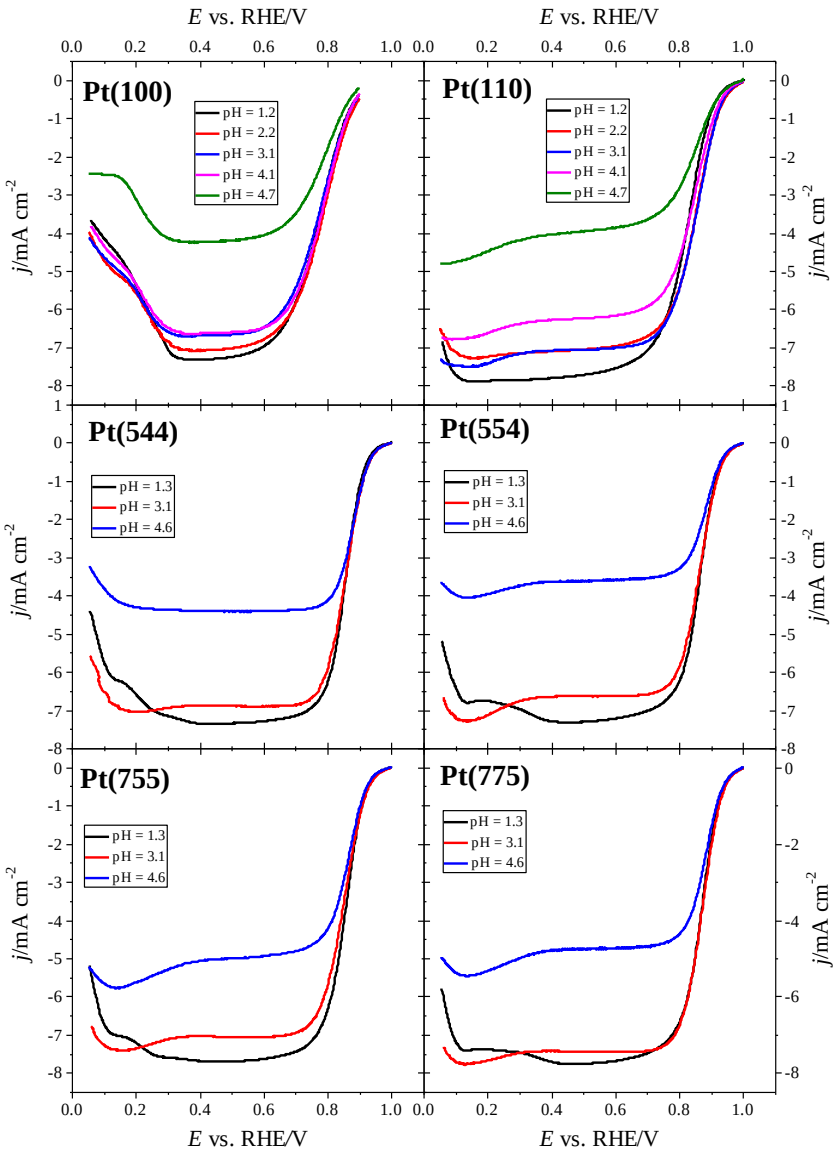


Fig. 6. Polarization curves for the ORR on different Pt orientations in $O_2$-saturated solutions with pH < 5 prepared with NaF/$HClO_4$ mixtures. Scan rate: 50 mV $s^{-1}$; rotation rate: 2500 rpm.

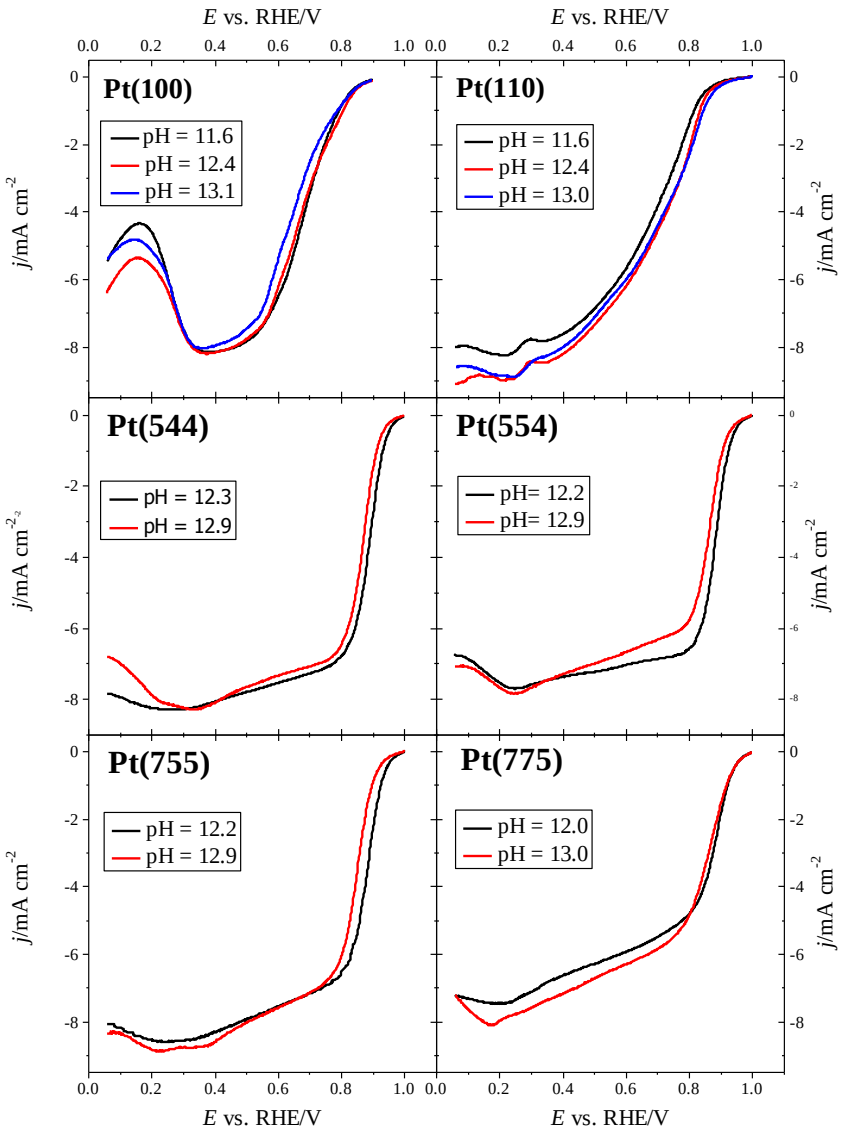


Fig. 7. Polarization curves for the ORR on different Pt orientations in $O_2$-saturated solutions with pH > 11 prepared with NaOH/$KClO_4$ mixtures. Scan rate: 50 mV $s^{-1}$; rotation rate: 2500 rpm.

*4.2.3. Kinetic analysis: kinetic current densities ($j_k$) and Tafel slopes*

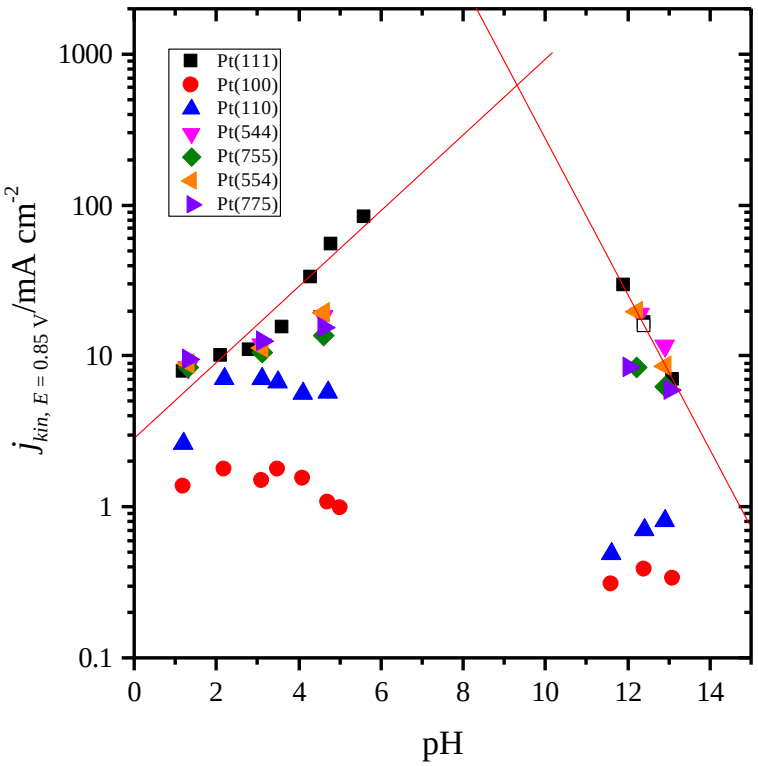


Fig. 8. Plot of the logaritm of $j_k$ at 0.85 V on the different Pt single crystal electrodes as a function of pH. The straight lines correspond to Pt(111). Open square correspond to Pt(111) in a NaOH/NaF mixture.

Although the polarization curves for the ORR shown above can provide a qualitative description of the effects of pH in the reaction, the quantitative analysis and the comparison between different pH values and surfaces require the calculation of the kinetic current density of the reaction calculated according to the procedures described in section 3.1. Fig. 8 shows the plot of $j_k$ at 0.85 V vs. pH for all the surfaces. As can be seen, a clear volcano curve is obtained for the Pt(111) surface. The linear fits obtained

for pH<6 and pH>11 cross at pH around 9, determining the point of maximum activity, that is, the maximum activity for this surface should be reached for pH values close to 9. Unfortunately, all the tested buffered solutions for pH around 9 contain species that adsorb on the electrode surface, and, this maximum cannot be corroborated experimentally.

The origin of this behavior for the Pt(111) electrode should be related to the interfacial properties, and more specifically to the potential of zero free charge. At the ORR onset potential, the surface is always covered by OH. In the case of acidic solutions, the onset is positive to the pztc of the electrode (0.28 V vs. SHE) (see figure 2). Assuming that the process of OH adsorption does not alter the value of the metal charge, this means that the electrode has a positive charge on the onset potential. On the other hand, in alkaline solutions, the onset is located at negative potentials with respect the pzfc, and thus the electrode surface should have a negative charge. According to the expected behavior, at pH=9, the onset potential lies in the region close to the pzfc, and in this pH value is where the maximum activity is obtained. As measured with the pulsed laser experiments, the pzfc is very close to the potential of maximum entropy [51, 64, 65], the region where the water layer close to the surface has the highest disorder. This disordered water layer facilitates then the reaction. It should be stressed that the potential for the OH desorption on the Pt(111) is not affected by the pH value, but, as shown in figure 1, the

OH adsorption isotherm is dependent on the pH, revealing the effects of metal charge and water structure on the process. These effects are also affecting the reactivity in this potential region. Another factor that could have an influence in the water structure (which also affects OH adsorption [28]) is the anions present in solution, since these solutions contains a mixture of fluoride, which is a kosmotropic anion, and $ClO_4^-$, a chaotropic anion. Possible effects of the interfacial water structure (which would change for the different Pt stepped surface at acidic pH values since they have different pzfc [18, 65]) were previously considered in the work of Bandarenka et al. [66]. Different solvation of the intermediates on (111) terraces on different stepped surfaces was also studied by Jinnouchi et al. by DFT computational methods in [67]. These results support the idea that the reactivity for the ORR of Pt surfaces can be enhanced by changing the interfacial water structure surrounding the intermediates.

The situation is completely different for the Pt(100) and Pt(110) electrodes. For these surfaces, the activity shows a slight monotonic diminution of the reactivity as the pH increases. The difference should be then related to the different OH adsorption strength and probably to the different water structure. For the Pt(111) surface, the onset potential for the reaction is in the region where the surface is covered by adsorbed OH. As the potential is made more negative, OH is progressively desorbed and at ca. 0.7 V (the region where the limiting diffusion current is observed) the OH coverage is almost negligible. From that potential value the ORR reaction is taking place in a free surface. This means that the adsorbed OH in the region of interest (between 0.7 and 1.0 V) is relatively labile. For the other two surfaces, the desorption of OH occurs at more negative potentials (around 0.3-0.5 V, for Pt(100) electrodes, [21]) and the ORR curve in the relevant region is recorded with a constant OH coverage. As the desorption occurs at low potentials for these electrodes, OH is strongly adsorbed on the surface in the region between 0.9 and 0.7 V, and probably, it is less affected by the electrode potential and water structure, giving rise to a constant behavior. A similar situation is observed for the Pt(110) electrode [68].

Stepped surfaces with (111) terraces show a mixed behavior between the Pt(111) and the other basal planes. In pH = 1.2, the behavior is the same as previously reported [12, 13]: higher activities are observed for narrower terraces. The (111) terrace should follow the same trend as the Pt(111) electrode, whereas the activity of the steps should remain almost constant with pH, as happens with the Pt(110) and Pt(100) electrodes. Thus, stepped surfaces also follow a volcano curve, but with gentler slopes. As expected, the increase in the acid region is dependent on the terrace width: the narrower the terrace is, the lower the increase in the region pH < 6 is observed. Thus, the increase in the current densities at 0.85 V as the pH increases in the acidic region for the Pt(554) or Pt(544) electrodes is larger than that observed for the Pt(775) or Pt(755) surfaces. In alkaline solutions, it should be stressed that the steps show negligible activity for the ORR in comparison with the terraces [15]. This observed behavior could explain the different trend in reactivity for stepped surfaces between acidic and alkaline media: while in acidic media the narrower the terraces are, the higher electrocatalytic activity is measured, in alkaline media surfaces with wider terraces are more electroactive [13, 15] due to the high dependence of the activity of the (111) plane with pH.

Another important parameter in the kinetics of the ORR is the Tafel slope. Tafel slopes were also calculated in the potential region around 0.85 V. The obtained results for Pt(111) and its vicinal stepped surfaces at pH values below 6 are around 65 mV/dec. In alkaline media, they slightly increase until reaching 71 mV at pH = 13.1. For the Pt(100) and Pt(110) electrodes, the values are higher than those measured for the Pt(111) surface. Higher dispersions are observed

with the Pt(110) electrode. It is known that this electrode undergoes reconstruction, which is very dependent on the annealing conditions [68]. Thus, small small differences in the flame-annealing treatment can lead to different surface structures and different slopes. The reported values for the Tafel slopes are in agreement with the previous works [1, 12, 13, 15, 29, 35]. As can be seen, Tafel slopes for each electrode are not strongly influenced by pH changes, implying that the reduction mechanism is not significantly affected by pH. It should be stressed that the Tafel slopes contains information not only on the rate determining step, but also on the changes of interaction between adsorbed species on the surface [15]. The constancy of these values suggests that the interaction between the species taking part in the mechanism and the surface are not affected by the pH changes.

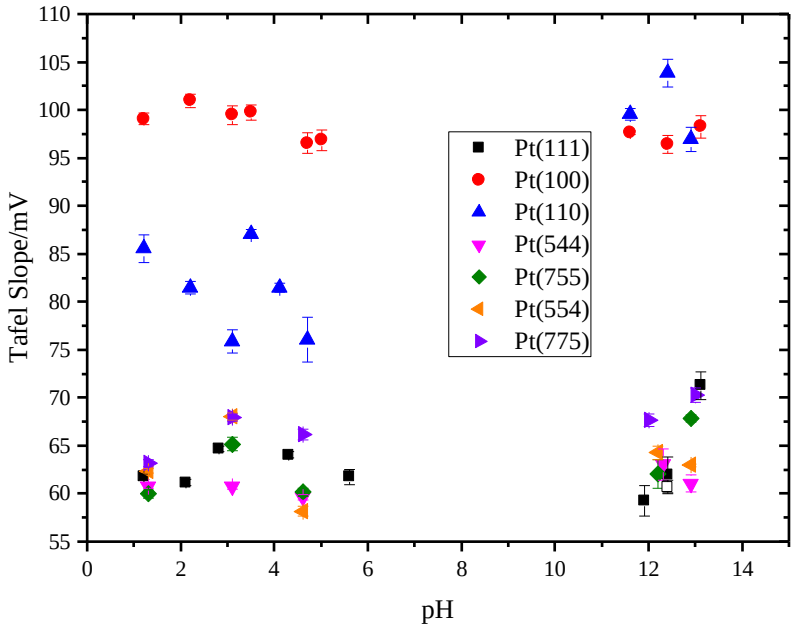


Fig. 9. Measured Tafel slopes for the different Pt single crystal electrodes as a function of pH. Open square correspond to Pt(111) in a NaOH/NaF mixture.

*4.2.4 On the variation of the limiting current while increasing the solution pH*

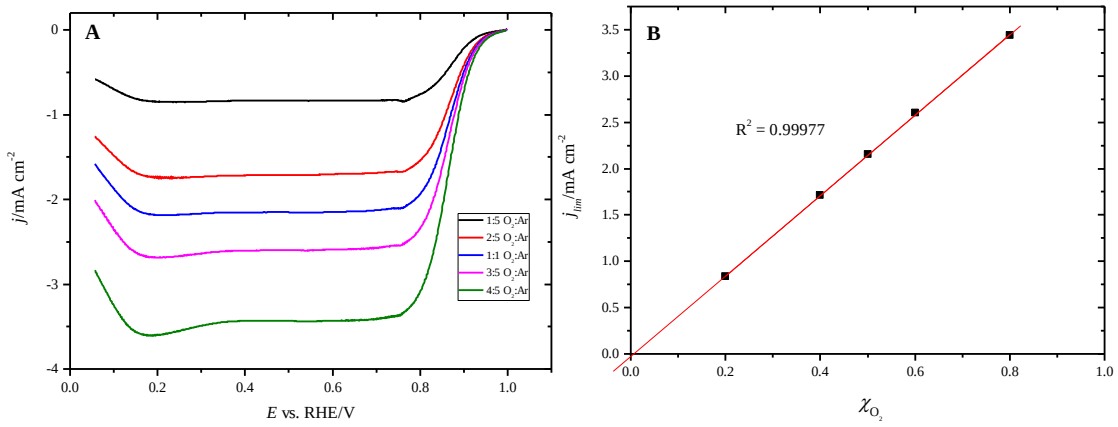

Fig. 10. ORR polarization curves for Pt(111) in a pH 4.1 solution prepared with a NaF/$HClO_4$ mixture and saturated with different $O_2$:Ar flow ratios (A), and $j_{lim}$ vs. $O_2$ molar fraction plot (B). Scan rate: 50 mV $s^{-1}$. Rotation rate: 1600 rpm.

The other remarkable and unexpected feature observed in Fig. 5 and Fig. 6 is the progressive decrease in the current density as the solution pH is increased from 1 to 6. One possibility for this phenomenon would be that a reaction involving $H_3O^+$ is limiting the reaction by diffusion control, analogously to previous observations for unbuffered solutions [60, 69, 70]. To confirm or discard this hypothesis, polarization curves using different concentrations of dissolved oxygen were recorded. The ratio of argon and oxygen in the gas flow bubbled to the solution was controlled with a mass flow controller. The chosen working solution was a NaF/$HClO_4$ mixture with pH ca. 4, in which the diminution of the limiting current is clearly noticeable. Fig. 10 shows the polarization curves for the different concentrations of oxygen, together with the plot of the limiting current density at 0.6 V vs. the molar fraction of oxygen. This dependency resulted to be perfectly linear, which indicates that the limiting reagent is oxygen and not $H_3O^+$. If $H_3O^+$ was limiting the oxygen reduction reaction by mass transport instead of $O_2$, the limiting currents would have been constant for all the $O_2$:Ar ratios, or at least

the plot would not be linear, if the limiting diffusion species changed with the $O_2$ concentration.

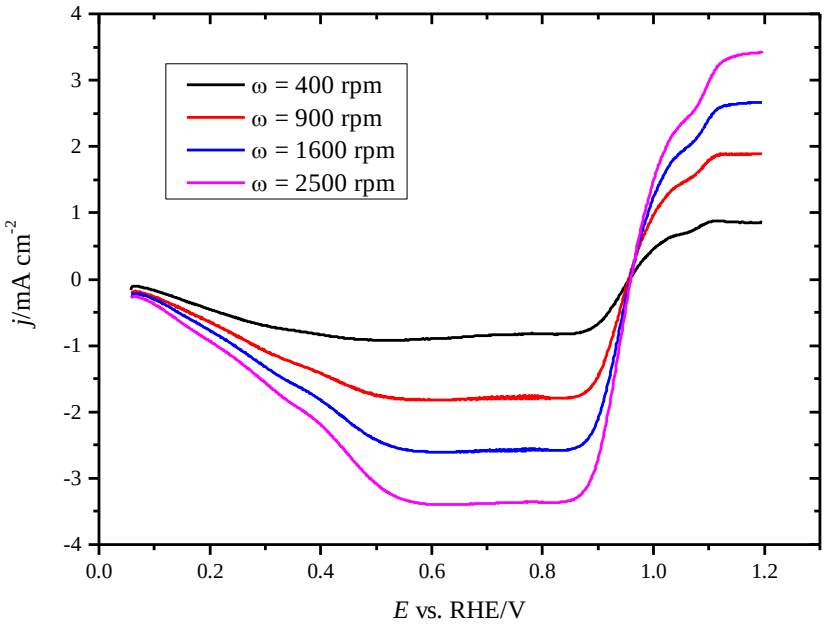


Fig. 11. HPOR and HPRR study on Pt(111) in a Ar saturated pH = 4.8 solution prepared with a NaF/$HClO_4$ mixture and 1 mM $H_2O_2$. Scan rate: 50 mV $s^{-1}$.

Hydrogen peroxide reduction and oxidation reactions (HPRR and HPOR) studies have been carried out in order to further corroborate that proton diffusion is not responsible of the observed effect. For the HPOR, in acidic conditions, hydrogen peroxide is the only reagent and $H^+$ is a product of the reaction. Under these conditions, proton diffusion has no effect on the outcome of the reaction. For the HPRR, proton and hydrogen peroxide are the reactants. If the limiting current density for the HPRR is the same that the one for the HPOR, it indicates that the diffusion of the proton is not a limiting reaction for the reduction. In order to check that, $H_2O_2$

reduction was studied on Pt(111) in a solution of pH ca. 5. As can be seen in Fig. 11, both limiting currents for the HPRR and HPOR are the same at pH = 4.8. In addition, only one wave is observed for the HPRR. As can be seen in the work of Strbac [69], HPRR measurements performed at more neutral values in unbuffered conditions show two waves because of the proton diffusion control, in a similar way to the observed by Li et al. with the oxygen reduction reaction [60]. This fact seems to indicate that, in the conditions presented here, solutions have enough buffer capacity to provide a correct proton

transport. For further corroboration of this hypothesis, HPRR and HPOR have been studied with a $H_2O_2$ concentration that produces the same limiting current density that the one measured for the ORR in an oxygen saturated solution (Fig. 12). Limiting current density obtained for HPRR in both pH = 1.2 and pH = 4.8 are the same and equal to the theoretical limiting current density obtained for the ORR in pH = 1.2. Moreover, the measured limiting current for the ORR at pH=4.8 is smaller than the one recorded for the HPRR at the same pH vale. This fact demonstrates that the solutions have enough buffering capacity for the reaction, and that the decrease for the ORR limiting current density for the ORR at more neutral values should then have another reason.

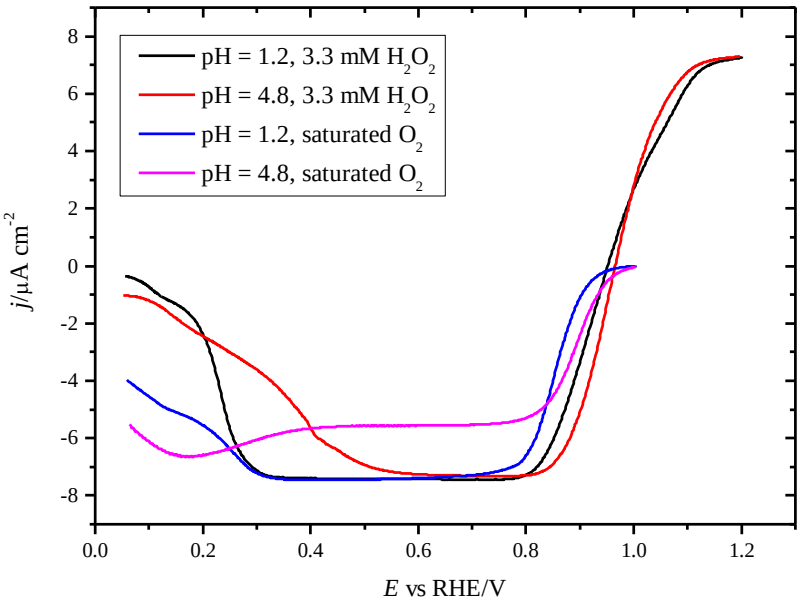


Fig. 12. Comparison between the ORR and the HPRR/HPOR at different pH values for the same limiting current density. Scan rate: 50 mV $s^{-1}$. Rotation rate: 2500 rpm.

Another possible explanation for the decrease in $j_{lim}$ would be that a fraction of the reacting oxygen produces hydrogen peroxide as final product instead of water, with the subsequent loss of faradaic efficiency. This only can be possible if hydrogen peroxide cannot be further reduced to water at high potentials in these conditions. In Fig. 11, it can be observed that hydrogen peroxide is fully reduced at potentials very close to 1.0 V and the limiting currents are the same as measured in 0.1 perchloric acid solution [71]. Thus, hydrogen peroxide should be reduced to water at potentials near to the onset potential of the ORR also at neutral pH values. An additional proof of this can be obtained using a rotating polycrystalline platinum ring-disk electrode, because the diminution of the limiting current is observed for all the surfaces, and also for the polycrystalline electrodes. In this case, experiments were performed for pH > 4.

The platinum ring was fixed at 1.1 V vs RHE to oxidize the possible generated hydrogen peroxide on the platinum disk electrode. Disk currents for pH = 4.5 follow the expected trend and they are lower than those measured for pH = 1.2, but, as can be seen in Fig. 13, hydrogen peroxide follows the same behavior in both pH values, while the ratio between ring and disk currents remains constant. These experiments further confirm that hydrogen peroxide is not responsible of the diminution of the limiting current observed for ORR at neutral pH values; e.g. once hydrogen peroxide is formed, it would be readily reduced.

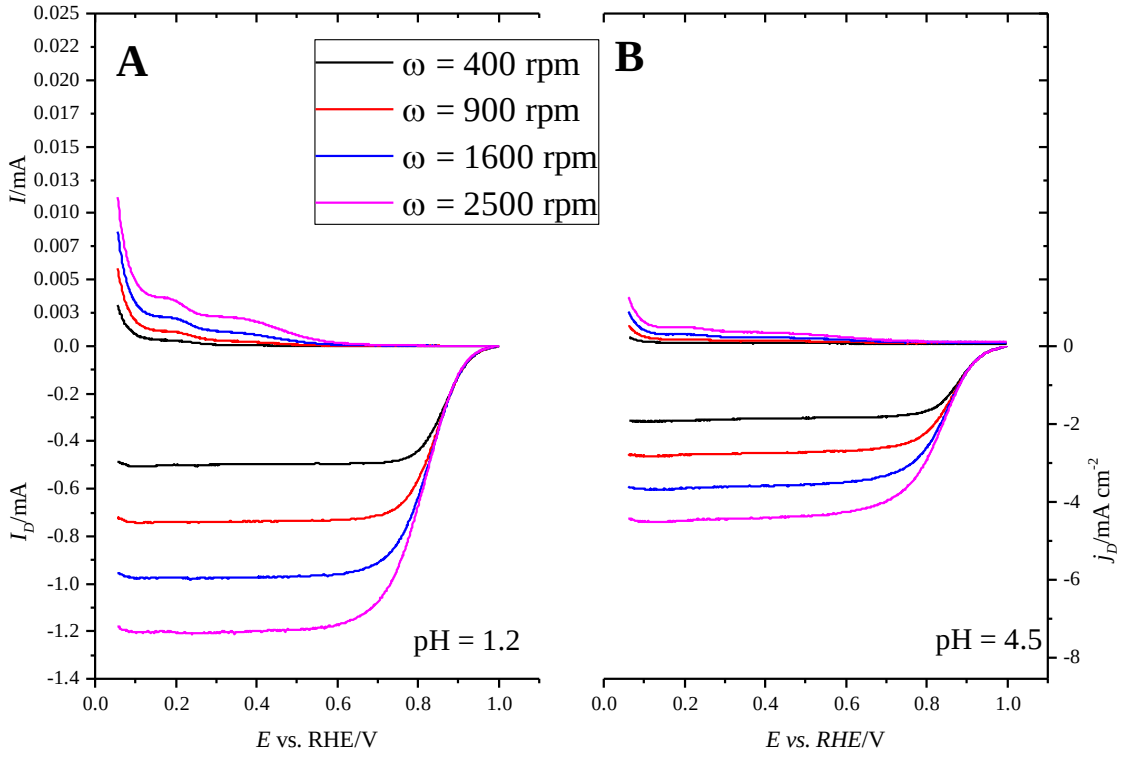


Fig. 13. RRDE experiments performed for the ORR on polycrystalline Pt in $O_2$ saturated pH 1.2 (A) and pH = 4.5 (B) solutions at different rotation rates. Pt-disk potential was fixed at 1.1 V. Scan rate: 50 mV $s^{-1}$

The diminution in the limiting current with pH should then have another cause. It can be proposed that the diminution of the limiting current is due to a bifurcation point in which a reaction intermediate, previous to peroxide formation, stops reacting electrochemically, having thus a loss of faradaic efficiency. In the light of the results and accordingly to [35], the general mechanism shown in Fig. 14 is proposed. According to this mechanism, $OOH^{\cdot}$ intermediate would be the key species in the bifurcation point of the ORR. The existence of adsorbed OOH intermediate formed via reaction (2) as a bifurcation point has been proposed previously [33, 34], but in the light of the results presented by Gómez-Marín et al. in [35], we consider that $OOH^{\cdot}$ can also be a soluble intermediate, existing an equilibrium between the adsorbed species and OOH in solution. For neutral pH values, via (reaction f2, fig. 14) would occur partially, and some of the $OOH^{\cdot}$ would diffuse to the bulk solution (reaction f1, fig. 14), where it would slowly disproportionate into oxygen and water through a bimolecular reaction, with the subsequent diminution in the number of transferred electrons and therefore the diminution of the limiting current. For more acidic pH values or for higher overpotentials (since at pHs around 4 the current

density returns towards the theoretical values at E < 0.4 V vs. RHE, see figure 5A), via (reaction f2, fig. 14) is more favored, giving water as the final product and transferring the theoretical four electrons. Under these conditions, the presence of adsorbed hydrogen could favor the reduction of $OOH^{\cdot}$ towards $H_2O_2$, as pointed out by equilibrium (reaction f3) in Fig. 14. At more neutral values, the surface electrode charge is less favorable for the reduction of $OOH^{\cdot}$, even using $H_{ads}$, It should be pointed out that the change of the water structure caused by the presence of the fluoride anion might also affect this reaction. Further work is required to clarify this issue.

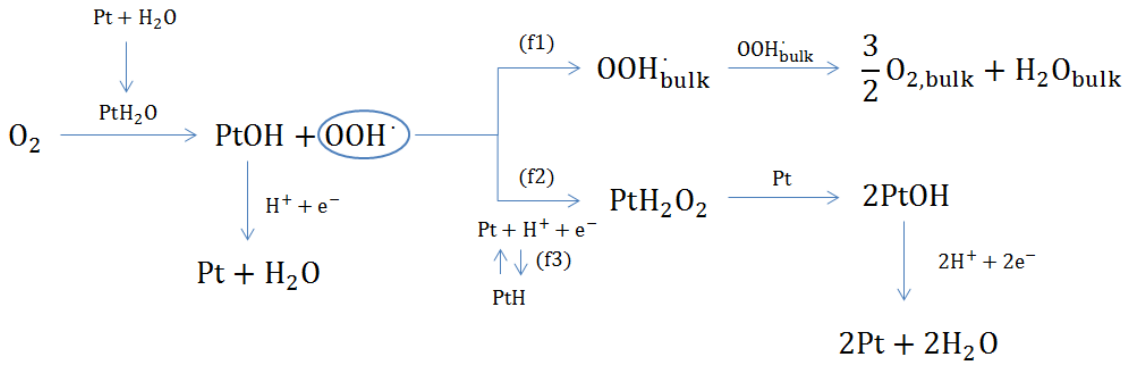


Fig. 14. Proposed mechanism for the ORR in acidic to neutral pH values.

## 5. Conclusions

In this work, we have demonstrated that oxygen reduction reaction at platinum single crystal electrodes can be studied for pH values as high as 6 in absence of specific anion adsorption and with suitable buffering capacity, by using NaF/$HClO_4$ mixtures with sufficiently high concentration. The plot of $j_k$ measured for the ORR vs. pH for the Pt(111) electrode follows a volcano curve whose extrapolated maximum is located around pH = 9. For this pH value, the reaction would face the ideal conditions regarding the electrode charge and the amount of adsorbed intermediates. A change in water structure determined by kosmotropic or chaotropic effects of the anions present in solution may have also some effect.

In the case of the other basal planes, Pt(100) and Pt(110), kinetic current densities are not affected the pH, while (111)×(111) and (111)×(100) stepped surfaces show an intermediate behavior: the larger the (111) terraces are, the higher the increase of the electrocatalytic activity as pH increases is. Tafel slopes are practically unaffected by changes in pH.

For all cases, and especially for Pt(111) and the stepped surfaces, a progressive decrease of the limiting current with increasing the pH is observed. The origin of this phenomenon can be related to a bifurcation in the mechanism previous to hydrogen peroxide formation, and originated probably by a soluble $OOH^{\cdot}$ intermediate, which in neutral pH values diffuses to bulk solution, implying a loss of faradaic current. It should be stressed that this work opens up the possibility of studying the electrocatalysis of different reactions at more neutral pH values, allowing a better understanding of the reactivity and the detection of intermediate species, like $OOH^{\cdot}$, which can be more stable and easier to detect in these neutral experimental conditions that could increase the lifetime of these intermediates near the electrode surface.

**6. Acknowledgments.**

This work has been financially supported by the MCINN-FEDER (Spain) and Generalitat Valenciana (Feder) through projects CTQ2016-76221-P and PROMETEOII/2014/013, respectively. VBM thankfully acknowledges to MINECO the award of a pre-doctoral grant (BES-2014-068176, project CTQ2013-44803-P).

**References**

[1] A.M. Gómez-Marín, R. Rizo, J.M. Feliu, Oxygen redution reaction at Pt single crystals: a critical overview, Catal. Sci. Technol., 4 (2014) 1685-1698.

[2] A.J. Appleby, Electrocatalysis and Fuel Cells, Catalysis Reviews, 4 (1970) 221.

[3] J.K. Nørskov, J. Rossmeisl, A. Logadottir, L. Lindqvist, J.R. Kitchin, T. Bligaard, H. Jónsson, Origin of the Overpotential for Oxygen Reduction at a Fuel-Cell Cathode, J. Phys. Chem. B, 108 (2004) 17886-17892.

[4] S. Mukerjee, S. Srinivasan, M.P. Soriaga, J. McBreen, Role of Structural and Electronic Properties of Pt and Pt alloys on Electrocatalysis of Oxygen Reduction. An In Situ XANES and EXAFS Investigation, J. Electrochem. Soc., 142 (1995) 1409-1422.

[5] R.R. Adzic, Recent advances in the kinetics of oxygen reduction, in: J. Lipkowski, P.N. Ross (Eds.) Electrocatalysis, Wiley-VCH, New York, 1998, pp. 197-242.

[6] J. Greeley, I.E.L. Stephens, A.S. Bondarenko, T.P. Johansson, H.A. Hansen, T.F. Jaramillo, J. Rossmeisl, I. Chorkendorff, J.K. Nørskov, Alloys of platinum and early transition metals as oxygen reduction electrocatalysts, Nature Chem., 1 (2009) 552-556.

[7] I.E.L. Stephens, A.S. Bondarenko, U. Gronbjerg, J. Rossmeisl, I. Chorkendorff, Understanding the electrocatalysis of oxygen reduction on platinum and its alloys, Energy Environ. Sci., 5 (2012) 6744-6762.

[8] V.R. Stamenkovic, B. Fowler, B.S. Mun, G.F. Wang, P.N. Ross, C.A. Lucas, N.M. Markovic, Improved oxygen reduction activity on $Pt_3Ni(111)$ via increased surface site availability, Science, 315 (2007) 493-497.

[9] M.T.M. Koper, Thermodynamic theory of multi-electron transfer reactions: Implications for electrocatalysis, J. Electroanal. Chem., 660 (2011) 254-260.

[10] J. Rossmeisl, A. Logadottir, J.K. Nørskov, Electrolysis of water on (oxidized) metal surfaces, Chem. Phys., 319 (2005) 178-184.

[11] J. Greeley, J. Rossmeisl, A. Hellman, J.K. Nørskov, Theoretical trends in particle size effects for the oxygen reduction reaction, Z. Phys. Chem. (Muenchen, Ger.), 221 (2007) 1209-1220.

[12] M.D. Maciá, J.M. Campina, E. Herrero, J.M. Feliu, On the kinetics of oxygen reduction on platinum stepped surfaces in acidic media, J. Electroanal. Chem., 564 (2004) 141-150.

[13] A. Kuzume, E. Herrero, J.M. Feliu, Oxygen reduction on stepped platinum surfaces in acidic media, J. Electroanal. Chem., 599 (2007) 333-343.

[14] A.M. Gómez-Marín, J.M. Feliu, Oxygen reduction on nanostructured platinum surfaces in acidic media: Promoting effect of surface steps and ideal response of Pt(111), Catal. Today, 244 (2015) 172-176.

[15] R. Rizo, E. Herrero, J.M. Feliu, Oxygen reduction reaction on stepped platinum surfaces in alkaline media, Phys. Chem. Chem. Phys., 15 (2013) 15416-15425.

[16] A.N. Frumkin, O.A. Petrii, B.B. Damaskin, Potential of Zero Charge, Plenum, New York, 1980, pp. 221-289.

[17] G. Collins, M. Schmidt, G.P. McGlacken, C. O'Dwyer, J.D. Holmes, Stability, Oxidation, and Shape Evolution of PVP-Capped Pd Nanocrystals, J. Phys. Chem. c, 118 (2014) 6522-6530.

[18] V. Climent, N. Garcia-Araez, E. Herrero, J. Feliu, Potential of zero total charge of platinum single crystals: A local approach to stepped surfaces vicinal to Pt(111), Russ. J. Electrochem., 42 (2006) 1145-1160.

[19] N. Garcia-Araez, V. Climent, E. Herrero, J.M. Feliu, J. Lipkowski, Thermodynamic approach to the double layer capacity of a Pt(111) electrode in perchloric acid solutions, Electrochim. Acta, 51 (2006) 3787-3793.

[20] V. Climent, R. Gómez, J.M. Orts, A. Aldaz, J.M. Feliu, The potential of zero total charge of single-crystal electrodes of platinum group metals, The Electrochemical Society, Inc., Pennington, NJ, 1997, pp. 222-237.

[21] R.M. Arán-Ais, M.C. Figueiredo, F.J. Vidal-Iglesias, V. Climent, E. Herrero, J.M. Feliu, On the behavior of the Pt(100) and vicinal surfaces in alkaline media, Electrochim. Acta, 58 (2011) 184-192.

[22] R. Rizo, E. Sitta, E. Herrero, V. Climent, J.M. Feliu, Towards the understanding of the interfacial pH scale at Pt(111) electrodes, Electrochim. Acta, 162 (2015) 138-145.

[23] R. Martínez-Hincapié, P. Sebastián-Pascual, V. Climent, J.M. Feliu, Exploring the interfacial neutral pH region of Pt(111) electrodes, Electrochem. Commun., 58 (2015) 62-64.

[24] H.S. Frank, W. Wen, Ion-solvent interaction. Structural aspects of ion-solvent interaction in aqueous solutions: A suggested picture of water structure, Discussions of the Faraday Society, 24 (1957) 133-140.

[25] O.Y. Samoilov, A new approach to the study of hydration of ions in aqueous solutions, Discussions of the Faraday Society, (1957) 141-146.

[26] B.E. Conway, The solvation factor in specifity of ion adsorption at electrodes, Electrochim. Acta, 40 (1995) 1501-1512.

[27] B. Hribar, N.T. Southall, V. Vlachy, K.A. Dill, How ions affect the structure of water, J. Am. Chem. Soc., 124 (2002) 12302-12311.

[28] A. Berna, V. Climent, J.M. Feliu, New understanding of the nature of OH adsorption on Pt(111) electrodes, Electrochem. Commun., 9 (2007) 2789-2794.

[29] A.P. Sandoval-Rojas, A.M. Gómer-Marín, M.F. Suárez-Herrera, V. Climent, J.M. Feliu, Role of the interfacial water structure on electrocatalysis: Oxygen reduction on Pt(111) in methanesulfonic acid, Catal. Today, 262 (2016) 95-99.

[30] A. Damjanovic, V. Brusic, Electrode Kinetics of Oxygen Reduction on Oxide-free Platinum Electrodes, Electrochim. Acta, 12 (1967) 615-628.

[31] R. Jinnouchi, K. Kodama, T. Hatanaka, Y. Morimoto, First principles based mean field model for oxygen reduction reaction, Phys. Chem. Chem. Phys., 13 (2011) 21070-21083.

[32] H.A. Hansen, V. Viswanathan, J.K. Nørskov, Unifying Kinetic and Thermodynamic Analysis of 2 $e^-$ and 4$^-$ Reduction of Oxygen on Metal Surfaces, J. Phys. Chem. C, 118 (2014) 6706-6718.

[33] J. Staszak-Jirkovský, E. Ahlberg, I. Panas, D.J. Schiffrin, The bifurcation point of the oxygen reduction reaction on Au-Pd nanoalloys, Faraday Discuss., 188 (2016) 257-278.

[34] P.S. Ruvinskiy, A. Bonnefont, C. Pham-Huu, E.R. Savinova, Using Ordered Carbon Nanomaterials for Shedding Light on the Mechanism of the Cathodic Oxygen Reduction Reaction, Langmuir, 27 (2011) 9018-9027.

[35] A.M. Gomez-Marin, J.M. Feliu, New Insights into the Oxygen Reduction Reaction Mechanism on Pt(111): A Detailed Electrochemical Study, Chemsuschem, 6 (2013) 1091-1100.

[36] P.S. Rao, E. Hayon, Redox Potentials of Free Radicals. IV. Superoxide and Hydroperoxyl Radicals $\cdot O_2^-$ and $\cdot HO_2$, J. Phys. Chem., 79 (1975) 397-402.

[37] T.J. Schmidt, V. Stamenkovic, P.N. Ross, N.M. Markovic, Temperature dependent surface electrochemistry on Pt single crystals in alkaline electrolyte - Part 3. The oxygen reduction reaction, Phys. Chem. Chem. Phys., 5 (2003) 400-406.

[38] M.-h. Shao, P. Liu, R.R. Adzic, Superoxide Anion is the Intermediate in the Oxygen Reduction Reaction on Platinum Electrodes, J. Am. Chem. Soc., 128 (2006) 7408-7409.

[39] M. Yaguchi, T. Uchida, K. Motobayashi, M. Osawa, Speciation of Adsorbed Phosphate at Gold Electrodes: A combined Surface-Enhanced Infrared Absorption Spectroscopy and DFT study, Journal of Physical Chemistry Letters, 7 (2016) 3097-3102.

[40] C. Korzeniewski, V. Climent, J.M. Feliu, Electrochemistry at Platinum Single Crystal Electrodes, in: A.J. Bard, C. Zoski (Eds.) Electroanalytical Chemistry: A Series of Advances, CRC Press, Boca Raton, 2012, pp. 75-169.

[41] J. Clavilier, D. Armand, S.G. Sun, M. Petit, Electrochemical adsorption behaviour of platinum stepped surfaces in sulphuric acid solutions J. Electroanal. Chem., 205 (1986) 267-277.

[42] B. Lang, R.W. Joyner, G.A. Somorjai, LEED Studies of High Index Crystal Surfaces of Platinum, Surf. Sci., 30 (1972) 440.

[43] E. Herrero, J.M. Orts, A. Aldaz, J.M. Feliu, Scanning tunneling microscopy and electrochemical study of the surface structure of Pt(10,10,9) and Pt(11,10,10) electrodes prepared under different cooling conditions, Surf. Sci., 440 (1999) 259-270.

[44] N.M. Markovic, B.N. Grgur, C.A. Lucas, P.N. Ross, Surface electrochemistry of CO on Pt(110)-(1x2) and Pt(110)-(1x1) surfaces, Surf. Sci., 384 (1997) L805-L814.

[45] G.A. Attard, A. Brew, Cyclic voltammetry and oxygen reduction activity of the Pt{1 1 0}-(1 × 1) surface, J. Electroanal. Chem., 747 (2015) 123-129.

[46] A. Bard, L. Faulkner, Electrochemical Methods: Fundamentals and Applications, John Wiley & Sons, Inc., United States of America, 2001.

[47] J. Clavilier, A. Rodes, K. Elachi, M.A. Zamakhchari, Electrochemistry at platinum single-crystal surfaces in acidic media - hydrogen and oxygen-adsorption, J. Chim. Phys. Phys.-Chim. Biol., 88 (1991) 1291-1337.

[48] A.M. Gomez-Marin, J.M. Feliu, Oxide growth dynamics at Pt(111) in absence of specific adsorption: A mechanistic study, Electrochim. Acta, 104 (2013) 367-377.

[49] M.T.M. Koper, J.J. Lukkien, Modeling the butterfly: the voltammetry of (root 3 x root 3)R30 degrees and p(2x2) overlayers on (111) electrodes, J. Electroanal. Chem., 485 (2000) 161-165.

[50] T. Pajkossy, D.M. Kolb, On the origin of the double layer capacitance maximum of Pt(111) single crystal electrodes, Electrochem. Commun., 5 (2003) 283-285.

[51] P. Sebastián, R. Martínez-Hincapié, V. Climent, J.M. Feliu, Study of the Pt(111) | electrolyte interface in the region close to neutral pH solutions by the laser induced temperature jump technique, Electrochim. Acta, (2017) http://dx.doi.org/10.1016/j.electacta.2017.1001.1089.

[52] R. Gómez, J.M. Orts, B. Alvarez-Ruiz, J.M. Feliu, Effect of temperature on hydrogen adsorption on Pt(111), Pt(110), and Pt(100) electrodes in 0.1 M HClO4, J. Phys. Chem. B, 108 (2004) 228-238.

[53] V. Briega-Martos, E. Herrero, J.M. Feliu, Borohydride electro-oxidation on Pt single crystal electrodes, Electrochem. Commun., 51 (2015) 144-147.

[54] J. Clavilier, K. Elachi, A. Rodes, In situ characterization of the Pt(S)-[n(111) x (111)] electrode surfaces using electrosorbed hydrogen for probing terrace an step sites, J. Electroanal. Chem., 272 (1989) 253-261.

[55] J. Clavilier, K. Elachi, A. Rodes, In situ probing of step and terrace sites on Pt(S)-n(111)x(111) electrodes, Chem. Phys., 141 (1990) 1-14.

[56] A. Rodes, K. Elachi, M.A. Zamakhchari, J. Clavilier, Hydrogen probing of step and terrace sites on Pt(S)-[n(111) × (100)], J. Electroanal. Chem., 284 (1990) 245-253.

[57] M.J.T.C. van der Niet, N. Garcia-Araez, J. Hernández, J.M. Feliu, M.T.M. Koper, Water dissociation on well-defined platinum surfaces: The electrochemical perspective, Catal. Today, 202 (2013) 105-113.

[58] A.M. Gómez-Marín, J.M. Feliu, Thermodynamic properties of hydrogen–water adsorption at terraces and steps of Pt(111) vicinal surface electrodes, Surf. Sci., 646 (2016) 269-281.

[59] K. Schwarz, B. Xu, Y. Yan, R. Sundararaman, Partial oxidation of step-bound water leads to anomalous pH effects on metal electrode step-edges, Phys. Chem. Chem. Phys., 18 (2016) 16216-16223.

[60] M.F. Li, L.W. Liao, D.F. Yuan, D. Mei, Y.-X. Chen, pH effect on oxygen reduction reaction at Pt(111) electrode, Electrochim. Acta, 110 (2013) 780-789.

[61] N.M. Markovic, H.A. Gasteiger, P.N. Ross, Oxygen Reduction on Platinum Low-Index Single-Crystal Surfaces in Sulfuric-Acid-Solution - Rotating Ring-Pt(Hkl) Disk Studies, J. Phys. Chem., 99 (1995) 3411-3415.

[62] N.M. Markovic, H.A. Gasteiger, N. Philip, Oxygen reduction on platinum low-index single-crystal surfaces in alka line solution: Rotating ring disk(Pt(hkl)) studies, J. Phys. Chem. B, 100 (1996) 6715-6721.

[63] D. Strmcnik, K. Kodama, D. van der Vliet, J. Greeley, V.R. Stamenkovic, N.M. Marković, The role of non-covalent interactions in electrocatalytic fuel-cell reactions on platinum, Nature Chem., 1 (2009) 466-472.

[64] N. Garcia-Araez, V. Climent, J. Feliu, Potential-Dependent Water Orientation on Pt(111), Pt(100), and Pt(110), As Inferred from Laser-Pulsed Experiments. Electrostatic and Chemical Effects, J. Phys. Chem. C, 113 (2009) 9290-9304.

[65] N. Garcia-Araez, V. Climent, J.M. Feliu, Potential-dependent water orientation on Pt(111) stepped surfaces from laser-pulsed experiments, Electrochim. Acta, 54 (2009) 966-977.

[66] A.S. Bandarenka, H.A. Hansen, J. Rossmeisl, I.E.L. Stephens, Elucidating the activity of stepped Pt single crystals for oxygen reduction, Phys. Chem. Chem. Phys., 16 (2014) 13625-13629.

[67] R. Jinnouchi, K. Kodama, A. Nagoya, Y. Morimoto, Simulated Volcano Plot of Oxygen Reduction Reaction on Stepped Pt Surfaces, Electrochim. Acta, 230 (2017) 470-478.

[68] G.A. Attard, K. Hunter, E. Wright, J. Sharman, R. Martínez-Hincapié, J.M. Feliu, The voltammetry of surfaces vicinal to Pt{110}: Structural complexity simplified by CO cooling, J. Electroanal. Chem., (2016) http://dx.doi.org/10.1016/j.jelechem.2016.1010.1005.

[69] S. Strbac, The effect of pH on oxygen and hydrogen peroxide reduction on polycrystalline Pt electrode, Electrochim. Acta, 56 (2011) 1597-1604.

[70] M. Rouhet, S. Bozdech, A. Bonnefont, E.R. Savinova, Influence of the proton transport on the ORR kinetics and on the $H_2O_2$ escape in three-dimensionally ordered electrodes, Electrochem. Commun., 33 (2013) 111-114.

[71] A.M. Gomez-Marin, K.J.P. Schouten, M.T.M. Koper, J.M. Feliu, Interaction of hydrogen peroxide with a Pt(111) electrode, Electrochem. Commun., 22 (2012) 153-156.